www.sciencemag.org/cgi/content/full/science.aac6472/DC1

Supplementary Materials for

A GABAergic projection from the zona incerta to cortex promotes cortical neuron development

Jiadong Chen* and Arnold R. Kriegstein*

*Corresponding author. E-mail: jardongchen@gmail.com (J.C.); kriegsteina@stemcell.ucsf.edu (A.R.K.)

Published 1 October 2015 on *Science* Express
DOI: 10.1126/science.aac6472

This PDF file includes:

Materials and Methods

Fetal Tissue Collection and Acute Vibratome Slice Section

Postmortem human fetal tissue was collected from elective pregnancy termination specimens at San Francisco General Hospital. Tissue was obtained only with previous patient consent and in strict observance of legal and institutional ethical regulations. Research protocols were approved by the Committee on Human Research at the University of California, San Francisco. Gestational age was determined using fetal foot length. Modified transfer solutions (*20*) were used to improve cell survival. Tissue specimens were collected in oxygenated (5% CO2 / 95% O2) artificial CSF (aCSF) solution (pH 7.3 - 7.4, 290 – 300 mOsm) on ice and transferred to the lab within 2 hours.

Cortical slabs were embedded in 4% low melting point agarose (Fisher Scientific) and placed in ice-cold aCSF for sectioning containing (in mM): 110 Choline Cl, 2.5 KCl, 0.5 CaCl2, 7 MgCl2, 1.3 NaH2PO4, 25 NaHCO3, 10 glucose. 400 μm slice sections were obtained by vibratome (Leica VT1200S) and maintained in an incubation chamber in recovery and recording aCSF containing (in mM): 125 NaCl, 2.5 KCl, 2 CaCl2, 1.3 MgCl2, 1.3 NaH2PO4, 25 NaHCO3, 10 glucose, at room temperature.

Animals

Mice were housed and treated according to guidelines from the University of California, San Francisco (UCSF) Laboratory Animal Care and Use Committee. SST::Cre and Ai14 mice (C57BL/6) were obtained from Jackson Laboratories.

Electrophysiology, Electrical and Optical Stimulation

Chemicals were from Sigma unless otherwise noted. Mice were anaesthetized with avertin (2.5%), the brains were dissected rapidly after decapitation, and placed in ice-cold oxygenated sectioning aCSF. 300 μm sagittal cortical slice sections were obtained by vibratome and maintained in an incubation chamber with recovery and recording aCSF. During experiments, individual slices were transferred to a submerged recording chamber and continuously perfused with the recovery and recording aCSF (4.0 ml/min) at 30°C. Slices were visualized under a microscope (Olympus BX51WI) using infrared video microscopy and differential interference contrast optics. Fluorescent signals were obtained under GFP excitation bandpass filters (480 ± 20 nm) by a Mercury lamp (75 mW). Recordings were made with an Axon 700B patch-clamp amplifier and 1320A interface (Axon Instruments). Signals were filtered at 2kHz using amplifier circuitry, sampled at 10 kHz, and analyzed using Clampex 10.2 (Axon Instruments). The amplitudes of synaptic currents and the frequency of spikes (Fig. 4G, H) were analyzed using Clampfit 10.2 (Axon Instruments), the amplitude and frequency of spontaneous or miniature synaptic responses were analyzed using MiniAnalysis (Synaptosoft Inc.).

Patch electrodes were made from borosilicate glass capillaries (BF 150-86-10, Sutter Instruments) and pulled on a P-97 Micropipette Puller (Sutter Instruments) for a resistance in the range of 4 – 6 MΩ. The pipettes were tip- and back-filled with internal solutions containing (in mM): 125 K-gluconate, 10 KCl, 10 HEPES, 4 MgCl2, 4 Na2ATP, 0.4 Na4GTP, 0.5 EGTA, 0.5% Neurobiotin for whole-cell current-clamp recording; For whole-cell voltage-clamp recording: 135 CsCl, 10 HEPES, 4 Na2ATP, 0.4

Na4GTP, 0.5 EGTA, 10 QX-314, 0.5% Neurobiotin; For perforated patch recording: 70 Cs-gluconate, 70 CsCl, 10 HEPES, 4 MgCl2, 4 Na2ATP, 0.4 NaGTP, 0.5 EGTA, 0.02 Alexa fluor 488, Gramacidin (0.2 mg/ml); For cell-attached recording, recording electrodes were filled with aCSF. For Mg^{2+}-free aCSF, the aCSF solution was the same as recording and recovery aCSF except that 0 mM MgCl2 was added. During whole-cell recording, small depolarizing current pulses (50 ms duration, 50 ms interval, 100pA) were injected into the cell to facilitate neurobiotin labeling. For local drug application, drugs were pressure applied through a pipette (tip diameter 10-20 μm). All antagonists were bath applied.

Photostimulation was delivered by mercury lamp (75 mW) with a GFP excitation bandpass filter and light pulses were generated by Master-8 (A.M.P.I. Inc.) through a high-speed shutter (UNIBLITZ). The power density of the blue light (*43, 44*) was 8-12 $mW \cdot mm^{-2}$, measured with a power meter (Coherent Instruments). Electrical stimulation was delivered through an isolator (A.M.P.I.). Current pulses (100 μs, 0.05 Hz) were generated by Master-8 and applied through concentric electrodes (World Precision Instruments).

Ca^{2+} Imaging

Ca^{2+} imaging was performed using an epifluorescence microscope (Olympus BX51WI). Deep layer cortical neurons in acute human fetal cortical slices were bulk loaded with Oregon Green 488 BAPTA-1-AM (OGB-1 AM, 1 mM). Excitation light was applied through a GFP excitation bandpass filter from a Xenon arc light source. Light pulses were delivered from filterwheel and Smartshutter (Lambda XL, Sutter). A short light exposure (5 ms) and low sampling frequency (1 Hz) were used to avoid photo bleaching. Fluorescence signals were collected by Metafluor software. Relative changes in fluorescence were calculated and normalized against the baseline by $\Delta F/F$, where F is the baseline fluorescence intensity and ΔF is the change in fluorescence during drug application.

Stereotaxic Viral Injection

Neonatal pups (P 0-1) were anesthetized by hypothermia for 10 min and positioned in the head holder. Glass micropipettes (Wiretrol 5 mL, Drummond Scientific) were pulled by a Pipette Puller (Model 730, David KOPF Instrument) to a tip diameter of 40 μm, and beveled at an angle of 45° with a custom-built beveler. Injections were carried out by a custom-built stereotaxic injection rig, 50 – 100 nl AAV virus was injected locally to targeted brain regions. The posterior fontanelle was used to zero x (anterior-posterior) and y (medial-lateral) coordinates, and the skin surface to zero the z (depth) coordinate. The injection coordinates were (x,y,z, in milimeters): zona incerta (1.00, -0.65, -3.40).

AAV1-EF1α-DIO-ChR2-EYFP virus were obtained from University of the North Carolina (UNC) vector core. AAV1-EF1α-DIO-TeLC-2A-GFP vector was constructed and packaged into AAV virus serotype 1 by Virovek Inc.

Immunohistochemistry

Human brain tissue was fixed in paraformaldehyde (PFA, 4%) dissolved in phosphate-buffered saline (PBS) at 4°C over two nights. Cortical slabs were trimmed and embedded in 3% agarose. Vibratome-sliced sections (50-100 μm) were obtained and processed for antigen retrieval; Mice were deeply anaesthetized and perfused transcardially with 0.9% normal saline followed by 4% PFA. The brains were dissected and post-fixed in 4% PFA at 4°C overnight. Vibratome-sliced sections (50-100 μm) were obtained and GFP fluorescence was examined under an epifluorescence scope. Post recording, slice sections (300-400 μm) were fixed by 4% PFA overnight.

Brain sections were incubated for 24 hours at 4°C with primary antibodies followed by 24 hours at 4°C with the appropriate secondary antibodies (Molecular probes, Invitrogen). The blocking solutions used were PBS / 0.2% gelatin / 0.1% Triton X-100 / 10% goat serum. For acute slices sections post-recording, 0.5% Triton X-100 was used to increase the antibody penetration during primary antibody incubation. Dylight streptavidin-549 (Vector Laboratories) was added together with secondary antibodies to visualize the morphology of neurobiotin (Vector Laboratories) filled cells. Primary antibodies were: Mouse anti-Neurofilament 2H3 (DSHB, 1: 350), Mouse anti-NeuN (Milipore, 1:400), Chicken anti-GFP (Aves Labs, 1: 1000), Rabbit anti-vGat (Synaptic Systems, 1: 500), Rat anti-Ctip2 (Abcam, 1:500), Rabbit anti-Satb2 (Abcam, 1: 2000), and Rabbit anti-Somatostatin14 (Bachem, 1:500).

Confocal imaging and Analysis

Sections were mounted on glass slides (Fisher) with Aqua Ploy / Mount mounting medium (Polysciences). High magnification images were acquired using a Leica SP5 confocal microscope. Tile scan images (Figs. 1A and S3) were acquired using Leica built-in software. Images were processed and analyzed using ImageJ (Fiji, NIH) or Imaris software (Bitplane). For analysis of dendritic morphology, stack-images (z-stack interval: 2 μm) of neurobiotin labeled cortical neurons were taken, the sequence of images from the contralateral and ipsilateral hemisphere was randomized before analyzing (Microsoft Excel), apical and basal dendrites of individual cortical pyramidal neurons (Fig. 3E-H) were traced using simple neurite tracer, and quantified using Sholl analysis (Fiji, NIH) (*45, 46*).

Statistical analyses

Data are presented as mean ± s.e.m. Data distribution and statistical comparisons were done using unpaired Student's *t*-test or one-way ANOVA with post hoc Tukey test for multiple comparisons.

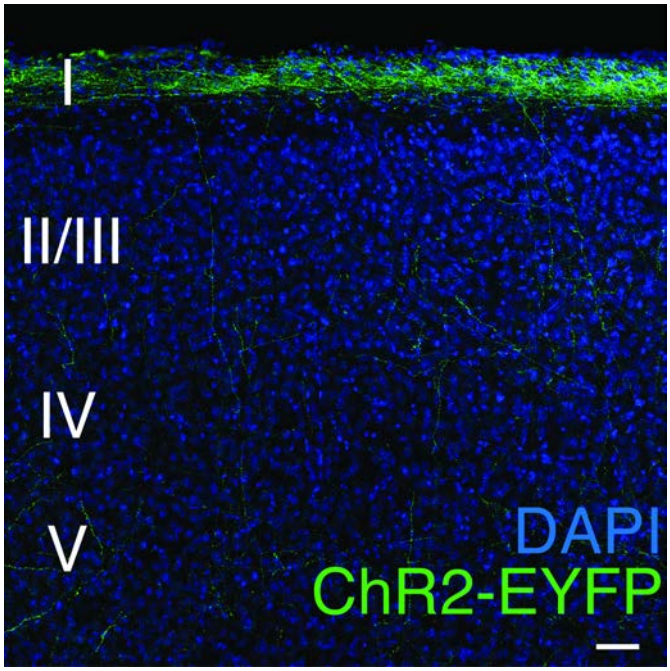

Fig. S1. GABAergic axons from the zona incerta project to cortical layer-1. Zoom-in image from Fig.1A showing the distribution of channelrhodopsin-2-EYFP expressing axons in layer-1 of somatosensory cortex.

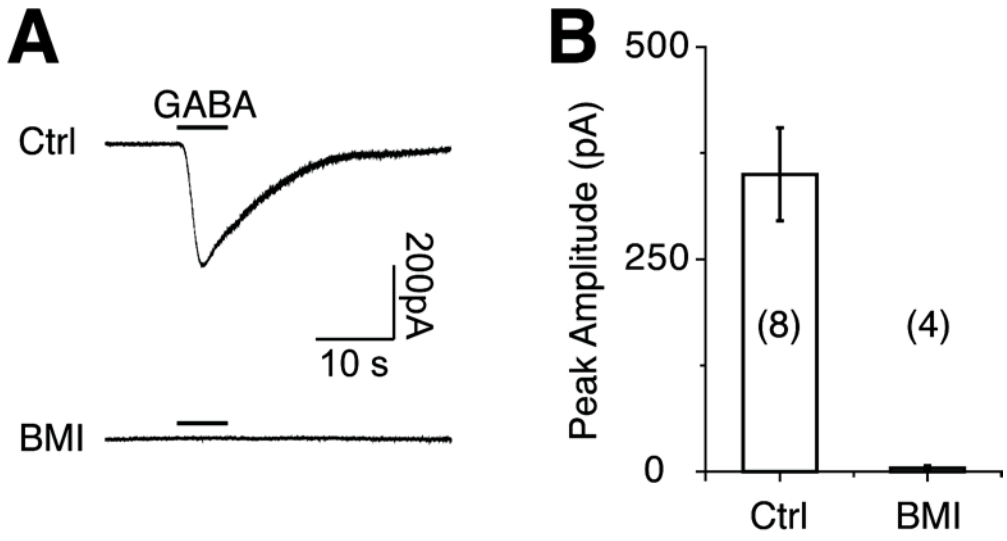

Fig. S2. Focal GABA-induced currents in human cortical neurons at GW 22. (**A**) Representative example and summarized result (**B**) showing GABA (100 μM) induced current is blocked by BMI (20 μM).

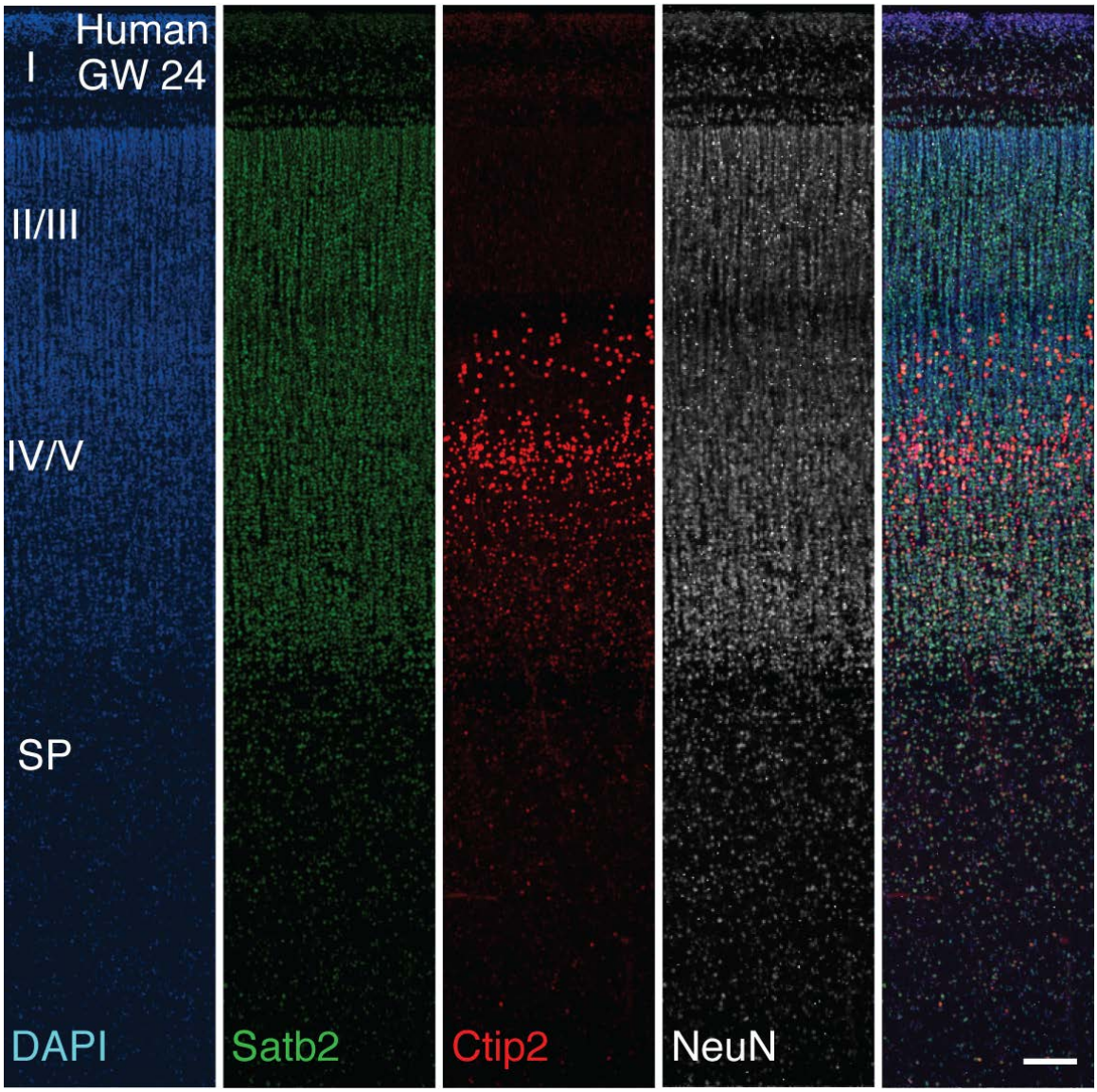

Fig. S3. Cortical layers in the human fetal cortex.
Cortical plate was identified by high density NeuN and DAPI markers. Regions with low density marker expression above and below the cortical plate are marginal zone (layer-1) and subplate (SP), respectively. Layer-4 and 5 were identified by the deep layer marker, Ctip2, whereas layer-2/3 was identified by the upper layer marker, Satb2. Note Satb2 is also expressed in layer-4 and 5 neurons at GW24. Scale bar: 100 μm.

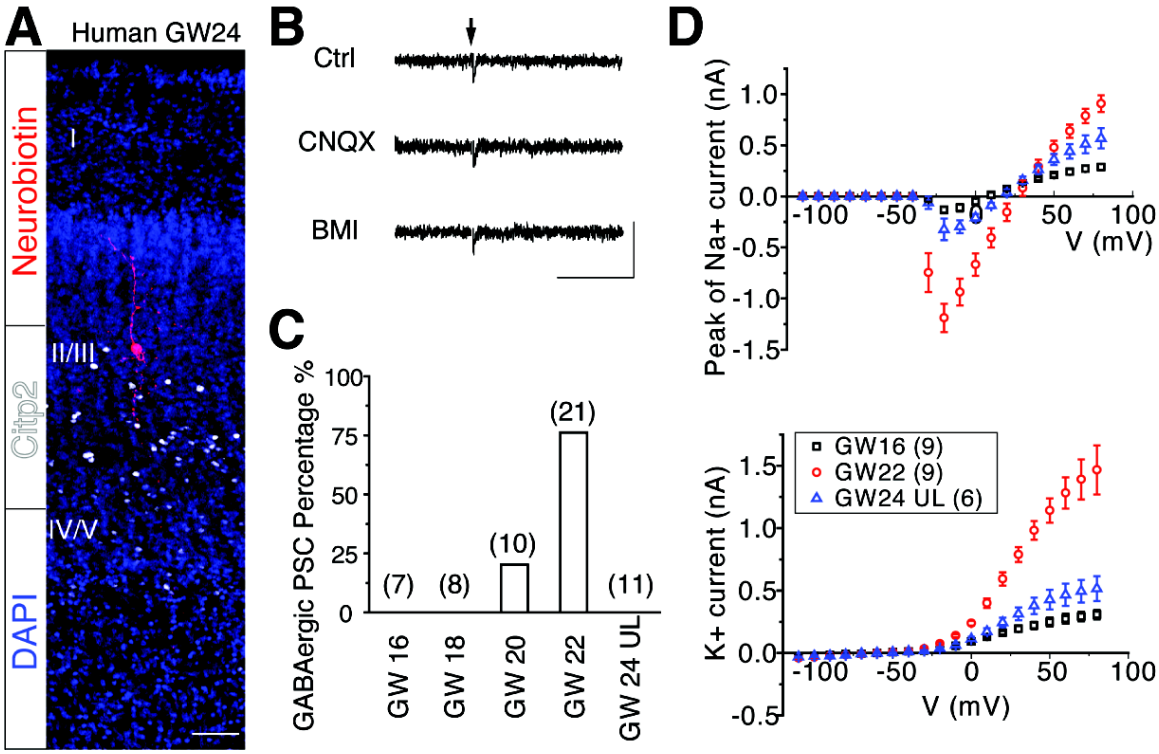

Fig. S4. Development of evoked GABAergic responses in human cortical neurons.

(**A**) Morphology of a recorded layer-2/3 cortical neuron intracellularly labeled with neurobiotin. Note the immature morphology of the apical dendrite. Ctip2, cortical layer-4 and 5 marker; DAPI, nuclear marker. (**B**) Electrical stimulation (arrow) of layer-1 did not induce synaptic currents in layer-2/3 neurons. (**C**) Percentage of cells receiving layer-1 stimulus-evoked synaptic inputs. Layer-5 neurons at GW16-22, layer-2/3 neurons at GW24. (**D**) Average voltage-gated Na^+ and K^+ currents of layer-5 neurons at GW16, GW22, and layer-2/3 neurons at GW 24. Scale bar: (**A**) 50 μm; (**B**) 50 pA and 50 ms.

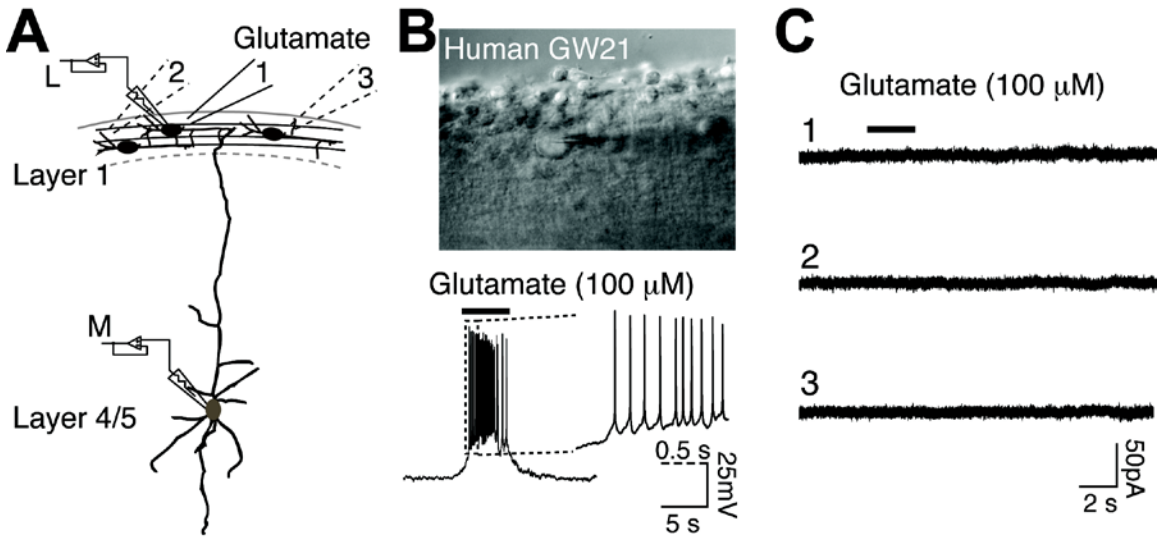

Fig. S5. Activating layer-1 local neurons did not evoke synaptic responses in layer-5 human cortical neurons.

(**A**) Schematic showing local application of glutamate to cortical layer-1. (**B**) Differential interference contrast (DIC) image showing whole-cell recording of layer-1 neurons and action potentials induced by local glutamate. (**C**) No synaptic responses were recorded in layer-5 neurons when applying glutamate locally at different locations in layer-1.

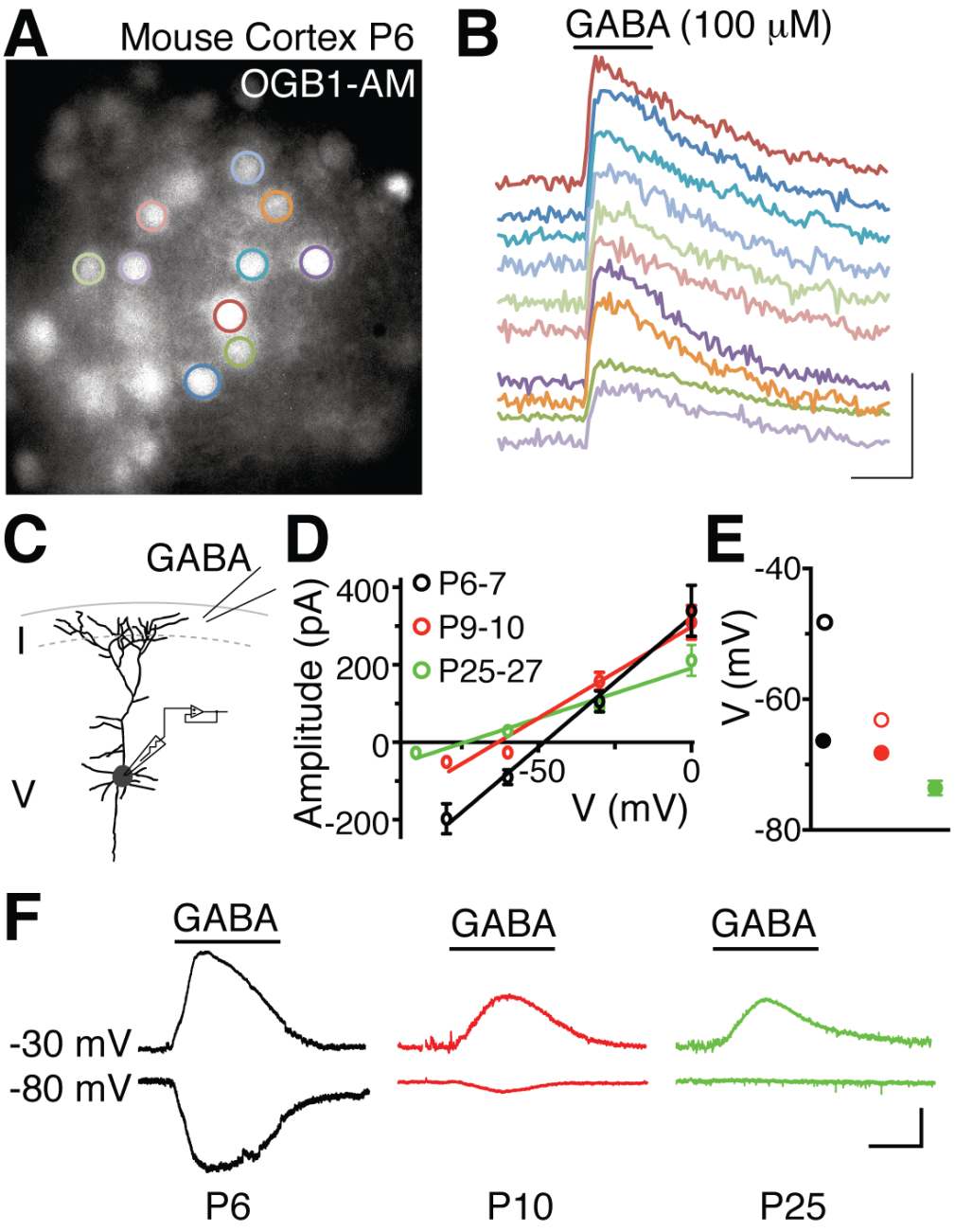

Fig. S6. GABAergic axons in neonatal mouse cortical layer-1.

(**A**) Bulk slice loading of Ca^{2+} indicator OGB1-AM in layer-5 mouse cortical neurons at P6. (**B**) Time-course of intracellular Ca^{2+} levels following local application of GABA. Color of the trace corresponds to color of the circled cell in panel **A**. (**C**) Schematic diagram shows perforated-patch recording of layer-5 neurons upon local GABA application in layer-1. (**D**) Statistical and representative (**F**) result showing reversal potential of layer-1 GABA induced currents in layer-5 neurons held at different membrane potentials. (**E**) GABA reversal potentials shift from depolarizing to hyperpolarizing in the postnatal mouse cortex. Open circles, GABA reversal potential at each stage were calculated by best-fit values from linear regression (P6-7: -48.1 mV, n =

10; P9-10: -63.2 mV, n = 13; P25-27: -74.0 mV, n = 8); filled circles, resting membrane potential (P6-7: -66.3 ± 0.7 mV, n = 47; P9-10: -68.2 ± 0.7 mV, n = 33; P25-27: -73.6 ± 1.1 mV, n = 17). Scale bars: (**B**) ΔF/F 50%, 20 s; (**F**) 100 pA, 5 s.

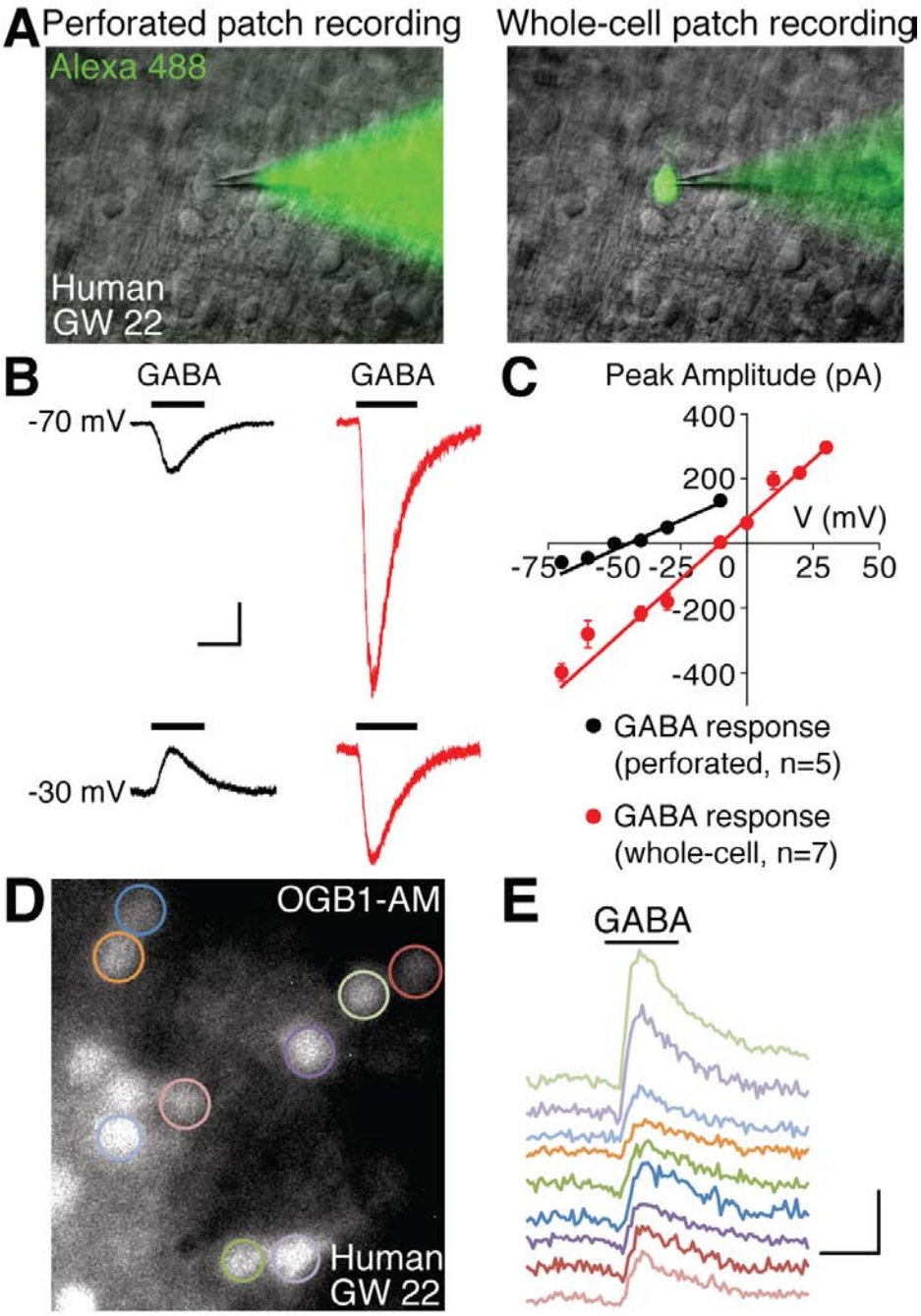

Fig. S7. GABA depolarizes human cortical neurons at GW 22.

(**A**) DIC image of a perforated patch recording with GFP fluorescence of Alexa 488 in the recording pipette. Dye is restricted to the pipette during perforated patch recording, but fills the recorded neuron when converted to whole-cell recording. (**B**) Local GABA (100 μM) induced responses in layer-5 cortical neurons at -70 mV or -30 mV, under perforated patch (black) or whole-cell patch (red) recording. (**C**) Statistical analyses showing the reversal potential of GABA-induced responses. (**D**) Bulk slice loading of Ca^{2+} indicator OGB1-AM in layer-5 human cortical neurons. (**E**) Time-course of

intracellular Ca^{2+} levels following local application of GABA. Color of the trace corresponds to color of the circled cell in panel **D**. Scale bar: (**B**) 50 pA, 5 s; (**E**) ΔF/F 50%, 20 s.

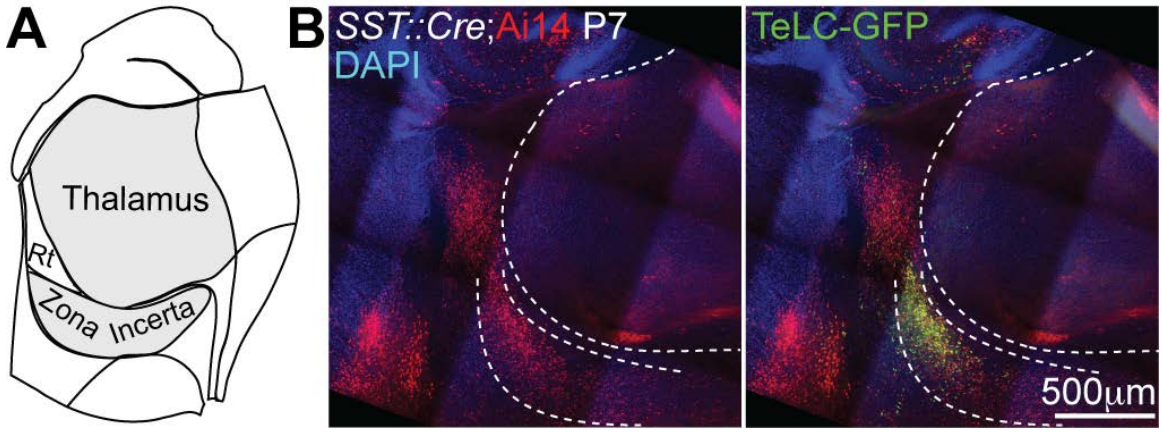

Fig. S8. Cluster of SST-expressing neurons in the ZI of developing mouse brain and specific labeling of the ZI SST neurons by stereotaxic injection.

(**A**) Schematic diagram shows the anatomy of the ZI region in the developing mouse brain as depicted in the developing mouse brain atlas (Allen Brain institute) and ref. (*47*). (**B**) Ai14 and TeLC-GFP expression in P7 *SST::Cre; Ai14* mice, with AAV1-DIO-TeLC-2A-GFP injected at P0-1.

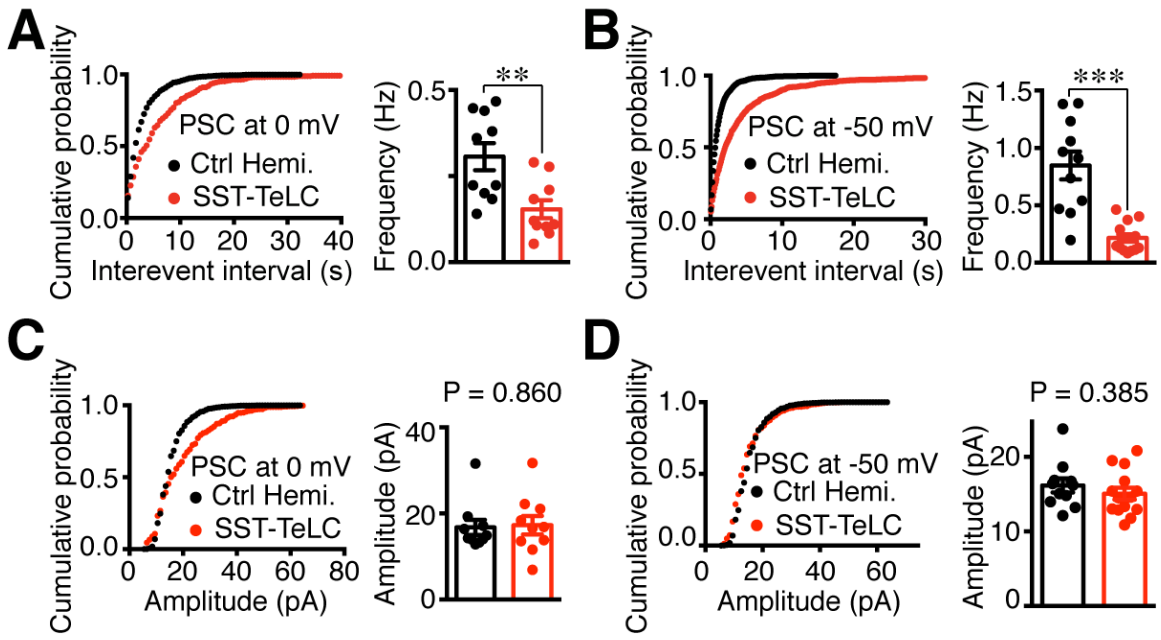

Fig. S9. The frequency, but not amplitude, of spontaneous postsynaptic currents is reduced in layer-5 neurons after selectively blocking ZI GABAergic transmission.

(**A**) Statistical results show reduced frequency of spontaneous GABAergic (at 0 mV) and glutamatergic (at -50 mV) responses (**B**) in layer-5 neurons one week after blocking ZI GABAergic transmission in neonatal SST::Cre mice (SST-TeLC). (**C, D**) The amplitude of spontaneous postsynaptic currents (PSCs) was unchanged (Unpaired *t*-test). (** $P < 0.01$; *** $P < 0.001$)

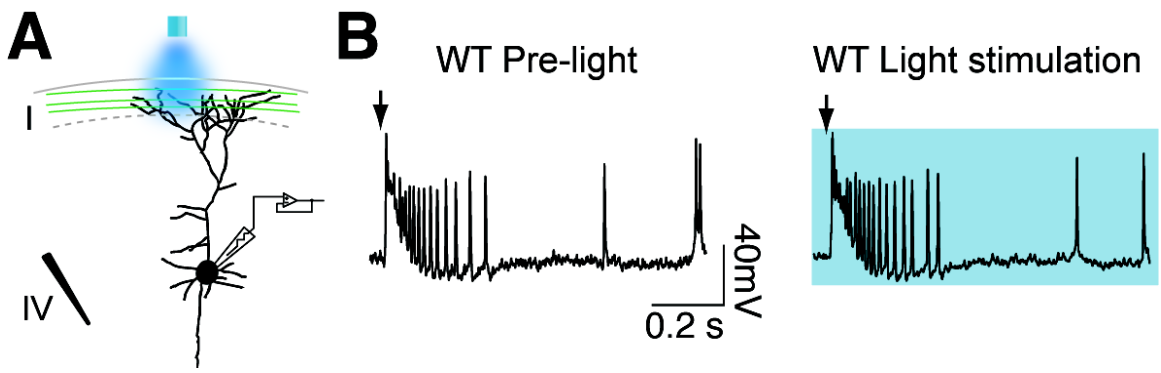

Fig. S10. Light stimulation did not affect epileptiform-like activity in wild-type mice.
(**A**) Schematic diagram shows intralaminar stimulation of layer-4 induces epileptiform-like activity in Mg^{2+}-free extracellular solution. Recorded in cell-attached mode. (**B**) Representative example shows epileptiform-like activity is not blocked by light stimulation in mice without ChR2 expression (wild type, WT).

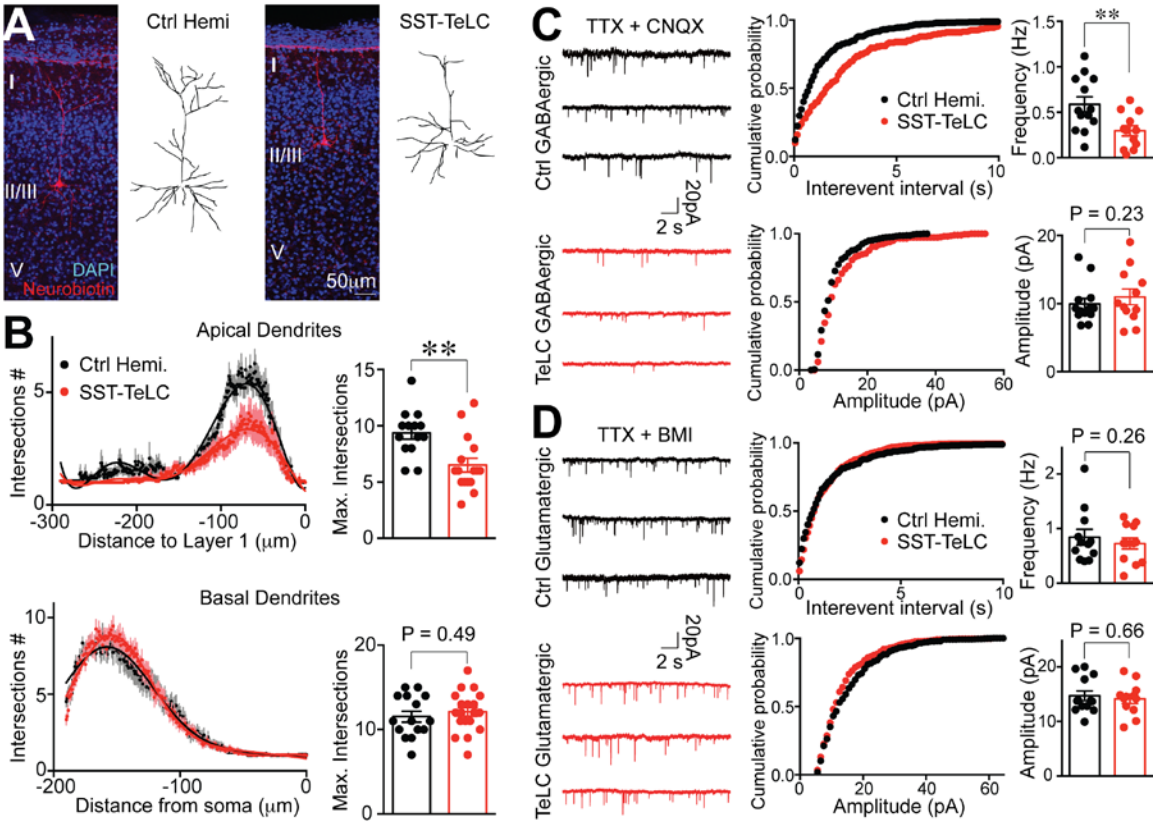

Fig. S11. Reduced GABAergic synaptic inputs and apical dendritic arbor complexity of layer-2/3 cortical neurons after blocking ZI GABAergic transmission.

(**A**) Neurobiotin-labeled and reconstructed morphology of layer-2/3 cortical pyramidal neurons (P9) after blocking ZI GABAergic transmission in neonatal SST::Cre mice (SST-TeLC). (**B**) Linear Sholl plots of apical and basal dendritic complexity of layer-2/3 cortical neurons (P7-10), showing best-fit polymonials (lines), average intersections (dots) and the s.e.m. (shaded regions). Statistical results show maximum number of intersections of dendritic arbors by Sholl analysis. (**C**) Reduced frequency, but not amplitude, of miniature GABAergic synaptic currents in layer-2/3 neurons recorded at -70 mV in the presence of TTX (1 μM) and CNQX (10 μM). (**D**) The frequency and amplitude of miniature glutamatergic synaptic currents remain unchanged in layer-2/3 neurons recorded at -70 mV in the presence of TTX (1 μM) and BMI (20 μM). Left panels in **C, D** show representative traces of 3 neurons in each group. (** $P < 0.01$. Unpaired *t*-test).

Author Contributions

J.C and A.R.K. conceived and designed the project, J.C. conducted experiments, analyzed data, and prepared the manuscript.